# A Turning-ray algorithm using Slotnick's equation

Babatunde Arenrin, Gary Margrave, and John Bancroft


## ABSTRACT

Turning-ray tomography is a good tool for estimating near surface velocity structure, especially in areas where conventional refraction statics fail such as in the case of a hidden layer. In a previous paper (Arenrin et al, 2014), we already demonstrated this by applying a tomostatics solution to Hussar 2D seismic line using Landmark's PROMAX software. In this paper we have developed a turning-ray tracing algorithm that uses Slotnick's equation. The algorithm traces turning rays through a linear velocity v(z) medium, and has the option of specifying the top layer velocity, takeoff angles, and the subsurface velocity gradient. However not in its final product, the turning-ray traveltimes from the algorithm are in agreement with the traveltimes generated using an acoustic finite-difference forward-modelling code.


## INTRODUCTION

Turning rays are continuously refracted arrivals due to the presence of a gradient that causes the rays to bend upward and return to the surface (Stefani, 1995). Ray tracing algorithms have been used to model traveltimes in turning-ray tomography studies. Stefani (1995) modelled first arrivals as turning rays in his paper on turning-ray tomography to seismic data from the Timbalier Trench in the Gulf of Mexico. Epili et al (2001) modelled turning rays and used turning-ray tomography to construct near surface velocity structure for a 2D dataset from Eastern Colorado. Zhu et al (1992) also modelled first arrivals as turning rays in their paper on turning-ray tomography and statics corrections.

First arrivals are usually modelled as refracted energy travelling along the interface between two layers and the model supports lateral changes in layer velocities (Zhu et al, 1992). In refraction studies, the subsurface velocities are derived from the slopes of the refracted signals. Several refraction methods exist to estimate subsurface velocities such as the intercept method, Hagedoorn plus-minus method, Generalised Reciprocal Method (GRM) and the Generalised Linear Inverse inversion (GLI), (Yilmaz, 2001). However in cases where velocity gradients exist within a layer, or the presence of a low velocity layer (LVL) between layers, modelling traveltimes as refracted energy could produce undesirable results, in other words, the traveltimes from a ray-tracing algorithm may not match the observed traveltimes. Modelling of traveltimes in the cases mentioned above could be done using turning-ray for better results.

## THEORY

Ray tracing is a method that applies the theories of how seismic waves travel within various mediums. The result of ray tracing gives an estimate of the distances travelled by the rays between reflection boundaries (Padina et al, 2006) or between sources and receivers in the presence of a velocity gradient. Several ray tracing techniques exist in literature such as the wavefront construction, fast marching methods, and grid ray tracing technique (Zhu et al, 2001).

Our approach to turning-ray tracing uses the analytical form of Slotnick's equations for a linear velocity v(z) medium. The equations are given as

$$x = \frac{1}{pc}\left\{\sqrt{1-p^2{v_0}^2} + \sqrt{1-p^2\left(v_0+cz\right)^2}\right\} \tag{1}$$

$$t = \frac{1}{c}\ln\left[\left(\frac{v_o+cz}{v_o}\right)\left(\frac{1+\sqrt{1-p^2{v_0}^2}}{1+\sqrt{1-p^2\left(v_0+cz\right)^2}}\right)\right], \tag{2}$$

where $x$ is the receiver location, $p$ is the ray parameter, $v_0$ is the top layer velocity, $c$ is the velocity gradient, $t$ is the traveltime of a ray from source to receiver and $z$ is the depth a ray has penetrated the subsurface at the receiver location.

Other types of ray tracing algorithms solve for $\mathbf{X}$ in Equation 3

$$\frac{d}{ds}\left[\mathbf{n}\frac{d\mathbf{X}}{ds}\right] = \nabla\mathbf{n}, \tag{3}$$

where $\mathbf{X}$ is the position along the ray, $s$ is the differential distance along the ray, and $\mathbf{n}$ is the slowness vector. A solution to $\mathbf{X}$ can be found in Langan et al (1985) or the use of wavefront ray tracing (wavefront tracing) by solving the eikonal equation (Equation 4) using finite-difference methods,

$$\left(\frac{\partial T}{\partial x}\right)^2 + \left(\frac{\partial T}{\partial y}\right)^2 + \left(\frac{\partial T}{\partial z}\right)^2 = n^2(x,y,z), \tag{4}$$

where $T(x,y,z)$ is the traveltime for a ray passing through a point $(x,y,z)$ in a medium with slowness $\mathbf{n}(x,y,z)$.

## METHOD

To model traveltimes through a linear velocity v(z) model using our algorithm, the following serve as inputs to the algorithm: the number of shots and their locations, the shot spacing, the receiver locations, the number of rays to shoot (which we usually take to be equal to the number of receivers), a one-dimensional slowness model, the minimum and maximum takeoff angles referred to as 'thetamin' and 'thetamax' respectively. The minimum and maximum takeoff angles control the maximum and minimum offsets for turning rays.

As mentioned previously, this method of turning-ray tracing using Slotnick's equation solves for z in Equation 1, calculates the lengths of raypaths from shots to receivers and builds the matrix of lengths of raypaths. The travel times are then computed using Equation (5) below,

$$\mathbf{t} = \mathbf{D}\mathbf{n}, \tag{5}$$

The $\mathbf{D}$ matrix is usually very sparse because not all the slowness cells are traversed by rays. Computing the inverse of the matrix $\mathbf{D}$ is not trivial especially with large scale problems. Solving for the slowness vector $\mathbf{n}$ is an inverse problem which has a least squares solution given as

$$\mathbf{n} = \left(\mathbf{D}^T\mathbf{D}\right)^{-1}\mathbf{D}^T\mathbf{t} \tag{6}$$

where $\mathbf{D}$ is the matrix of the lengths of raypaths, $\mathbf{n}$ is the slowness vector and $\mathbf{t}$ is the computed traveltime vector, and $\mathbf{D}^T$ is the matrix transpose.

The work presented here is based on the forward modelling by ray tracing. In a subsequent paper, we will solve the inverse problem of obtaining the slowness model vector using Equation (6). We should also mention that we have not used Equation 2 to calculate the traveltimes for the results presented here. In the future however, we will compare the results of the traveltimes using Equation 2 with the results of the traveltimes using Equation 5.

## EXAMPLE

In this section, we will show an example from the turning-ray tracing algorithm. Four synthetic shot records were generated using the acoustic finite-difference modelling code from the CREWES toolbox. The shot spacing is 20 meters and the receiver spacing is 2 meters. The velocity model for forward-modelling has a cell size of 2 meters by 2 meters and a dimension of 800X800 cells. The length of the shot record is 1 second.

For ray-tracing, the cell size is up scaled to 20 meters by 20 meters, given a dimension of 80X80cells. The minimum and maximum takeoff angles for turning rays are 40 and 75 degrees respectively. We find these takeoff angles adequate to trace rays to the nearest offset of about 452 meters. However, if we shoot rays beyond 75 degrees, we discover errors in the algorithm. Similarly if we shoot rays below 40 degrees, there won't be any receivers to capture the turning rays or the rays may not have the depth to turn upwards and be recorded at the receivers due to the size of our velocity model.

The linear velocity v(z) model for the shot records has a top layer velocity of 1800 m/s and a velocity gradient of 2.2/s.

Figure 1 below shows a shot record from an acoustic finite-difference forward-modelling code. We observe clearly the direct arrival and the turning ray.

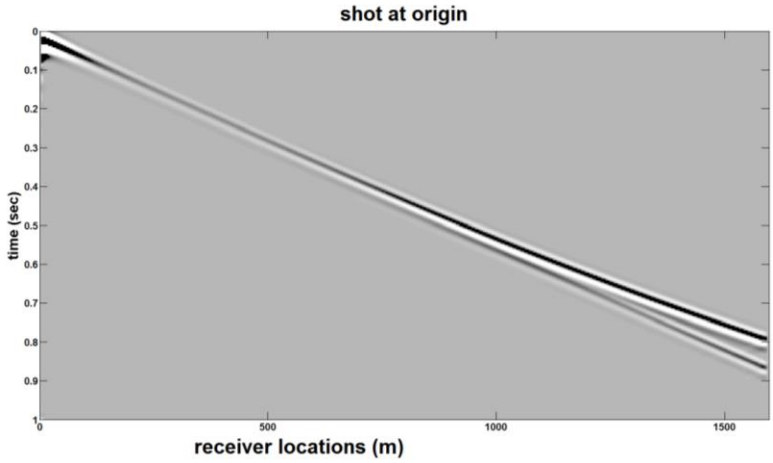


FIG 1. A shot record at the origin showing turning rays. Turning rays are modelled using an acoustic finite-difference algorithm.

Figure 2 below shows the same shot record as Figure 1. The plot in red is the traveltimes picked with an automatic picker. The plot in magenta is the traveltimes calculated using our ray tracing algorithm. We observe that the calculated traveltimes and the traveltimes from the automatic picker lie within the envelope of the turning ray from finite-difference modelling. The match is good in both cases.

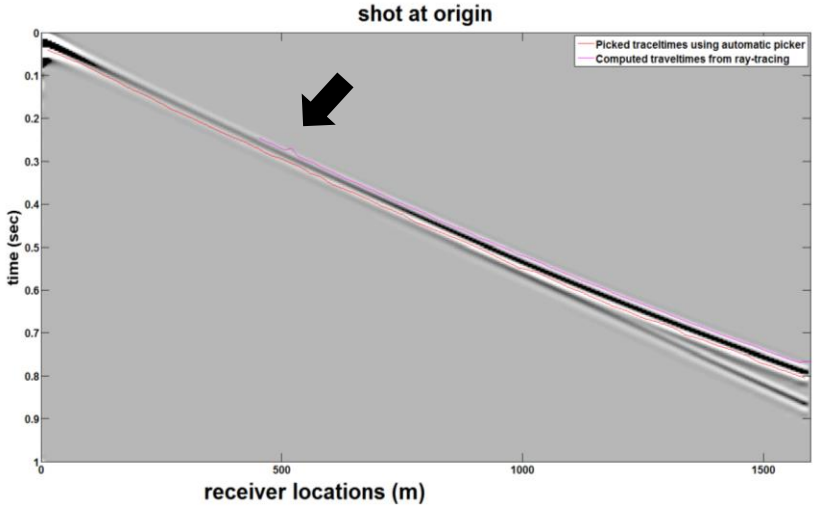


FIG 2. Shot record from FIG 1 with traveltimes plotted. Traveltimes from an automatic picker (red) and traveltimes calculated from ray tracing (magenta).

The black arrow in Figure 2 points to the region where the ray-tracing algorithm has errors. The errors may be due to errors in the extrapolation scheme used to extend the turning rays to the surface. These errors seem to be consistent across all four shots. The maximum offset for this shot is 1580 meters.

Figure 3 shows the turning rays from the shot at the origin to the receivers.

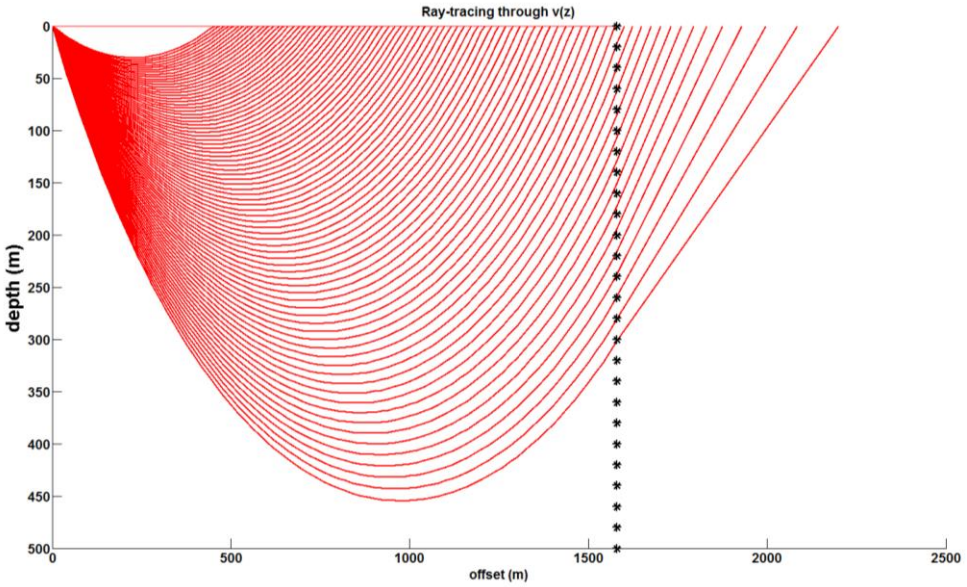


FIG 3. Modelling turning rays from the shot at the origin. The stared line is the position of the maximum offset for this shot (1580 meters).

Figure 4 below is the linear velocity used to generate the shot records and the traveltimes from ray tracing.

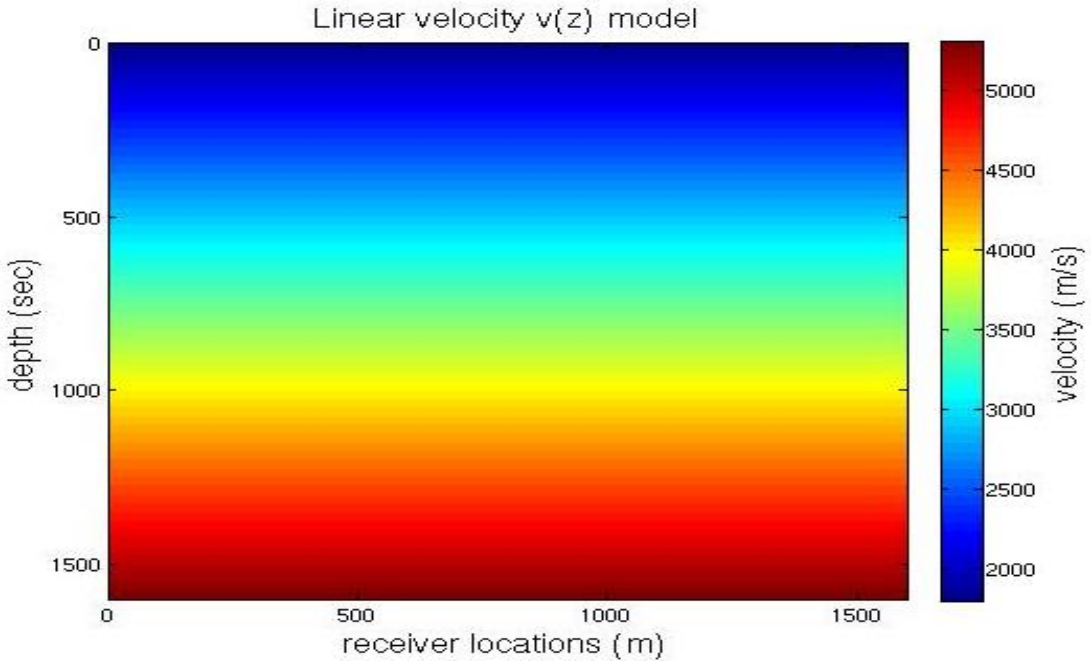


FIG 4. Linear velocity v(z) for ray tracing and the synthetic shot records. The velocity model is 1598 meters wide and 1598 meters deep.

Figure 5 below is a shot record from shot number 2 and the calculated traveltimes is displayed in magenta. The figure shows there is a good match between the traveltimes

from finite-difference modelling and the traveltimes calculated from the ray tracing algorithm.

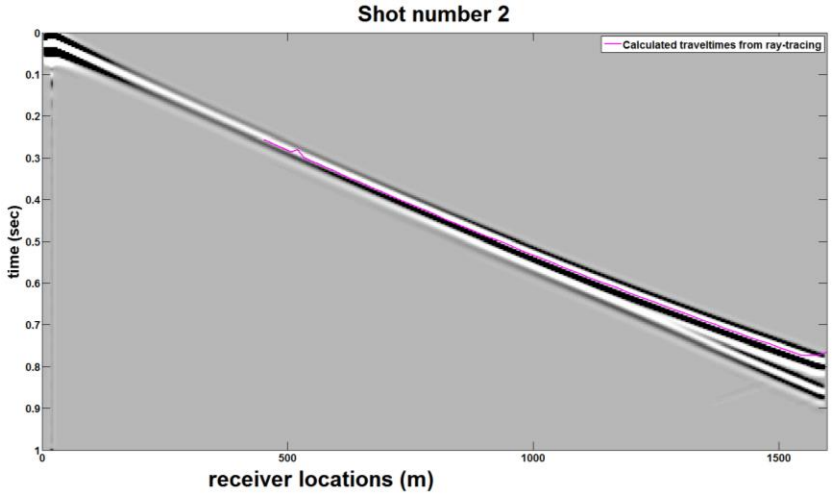


FIG 5. Shot record with traveltimes plotted. Traveltimes calculated from ray tracing (magenta) superimposed on the shot records.

Figure 6 shows the turning rays from shot number 2 (shot location is at 20 meters from the origin) to the receivers.

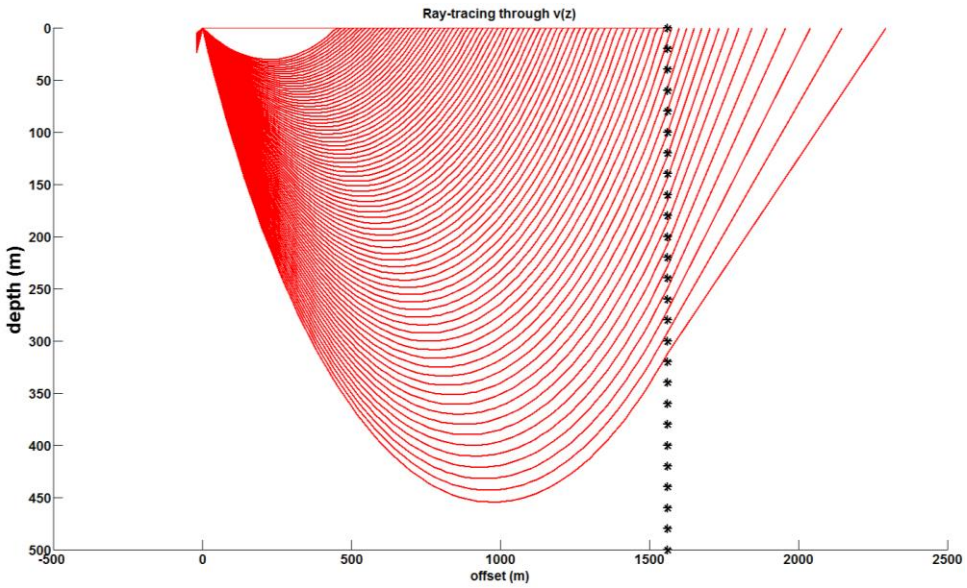


FIG 6. Modelling turning rays from shot number 2. The stared line is the position of the maximum offset for this shot (1560 meters).

Figure 7 below is a shot record from shot number 3 and the calculated traveltimes is displayed in magenta. We also observe that there is a good match between the traveltimes from finite-difference modelling and the traveltimes calculated from the ray tracing algorithm.

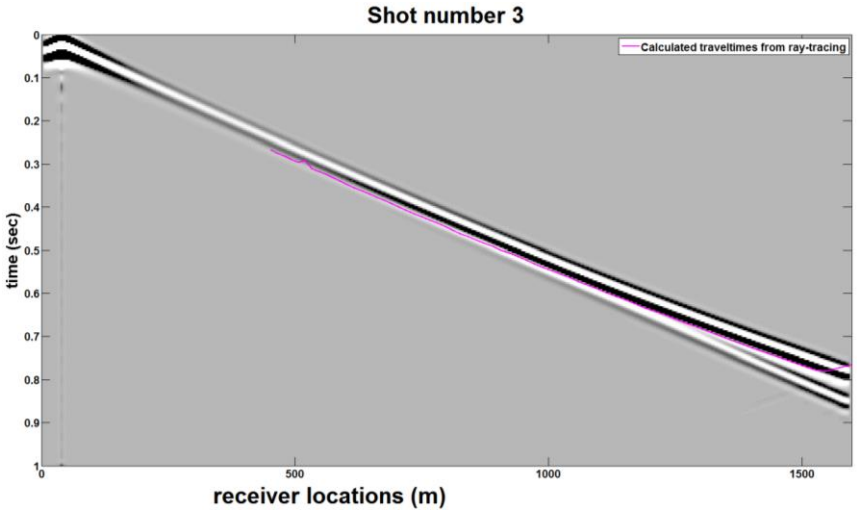


FIG 7. Shot record with traveltimes plotted. Traveltimes from ray tracing (magenta) superimposed on the shot records

Figure 8 shows the turning rays from shot number 3 (shot location is at 40 meters from the origin) to the receivers.

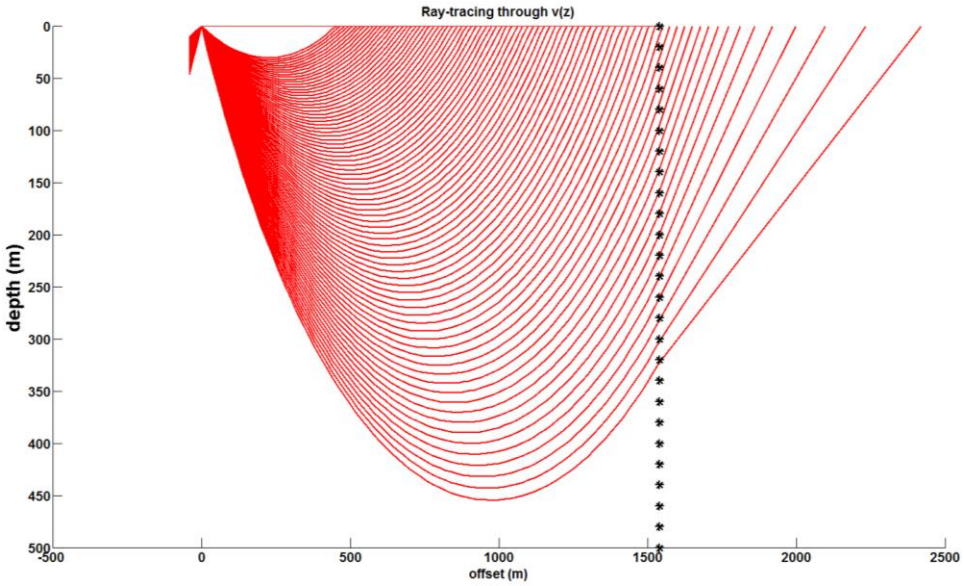


FIG 8. Modelling turning rays from shot number 3. The stared line is the position of the maximum offset for this shot (1540 meters).

For shots number 1, 2 and 3, we can see that the ray-tracing algorithm has done a good job in computing the traveltimes for the linear velocity v(z) medium.

Figure 9 below is a shot record from shot number 4 and the calculated traveltimes from ray tracing is displayed in magenta. Here we observe that there is a poor match between the traveltimes from finite-difference modelling and the traveltimes calculated from ray tracing especially at the nearer offsets.

However, we think this should not be a hitch if we want to solve the inverse problem of estimating the slowness (velocity) model because from our experience with industry software, modules for tomography or tomostatics come with the option of choosing the maximum traveltime residual to use in the inversion and/or the option to select what shots to use for the inversion. This serves as an effective way to condition the inversion.

The use of plot or display programs can help the user to identify what shots need to be dropped before inversion.

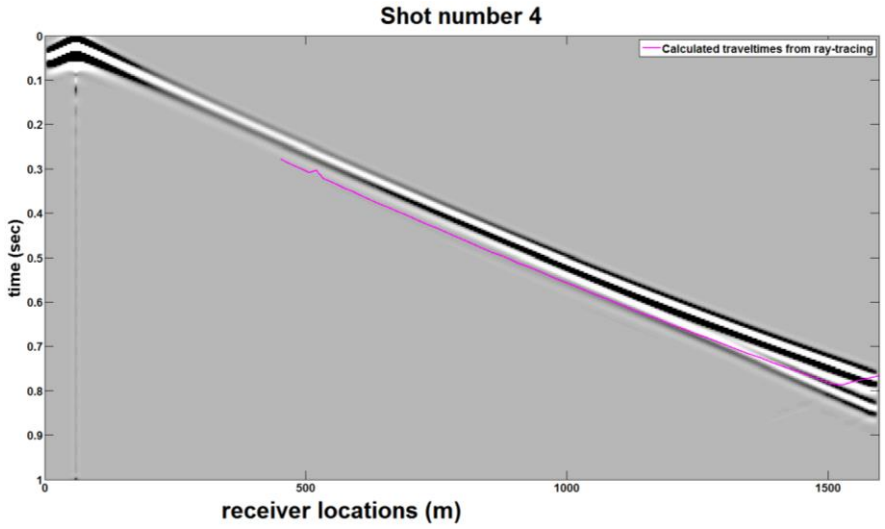


FIG 9. Shot record with traveltimes plotted. Traveltimes calculated from ray tracing (magenta) superimposed on the shot records.

Figure 10 shows the turning rays from shot number 4 (shot location is at 60 meters from the origin) to the receivers.

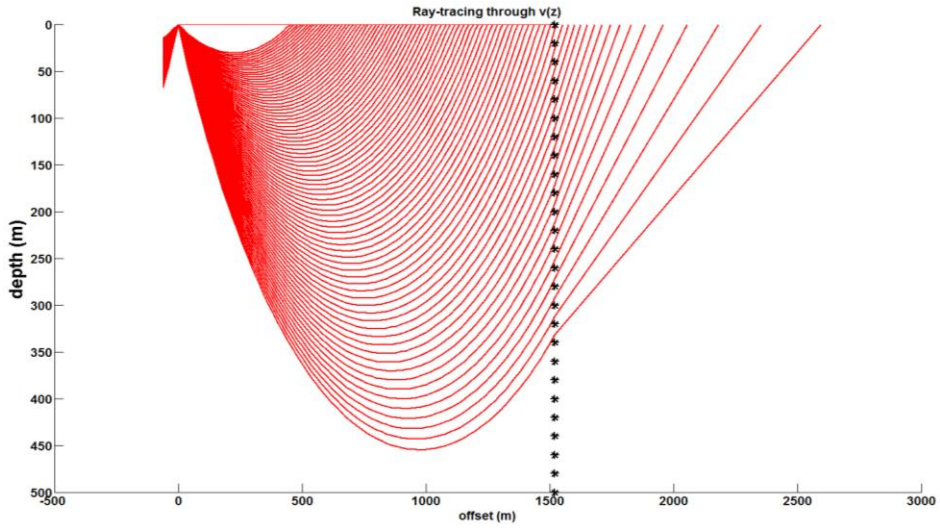


FIG 10. Modelling turning rays from shot number 4. The stared line is the position of the maximum offset for this shot (1520 meters).

The turning rays for all four shots displayed above show errors at offsets greater than the farthest offset in our synthetic shot records. Ideally these rays will not have been recorded at the receivers. However we extrapolated the rays to reach the surface (z=0).

Figures 11, 12, 13 and 14 show the matrices of the lengths of raypaths represented by **D** in Equation 5.

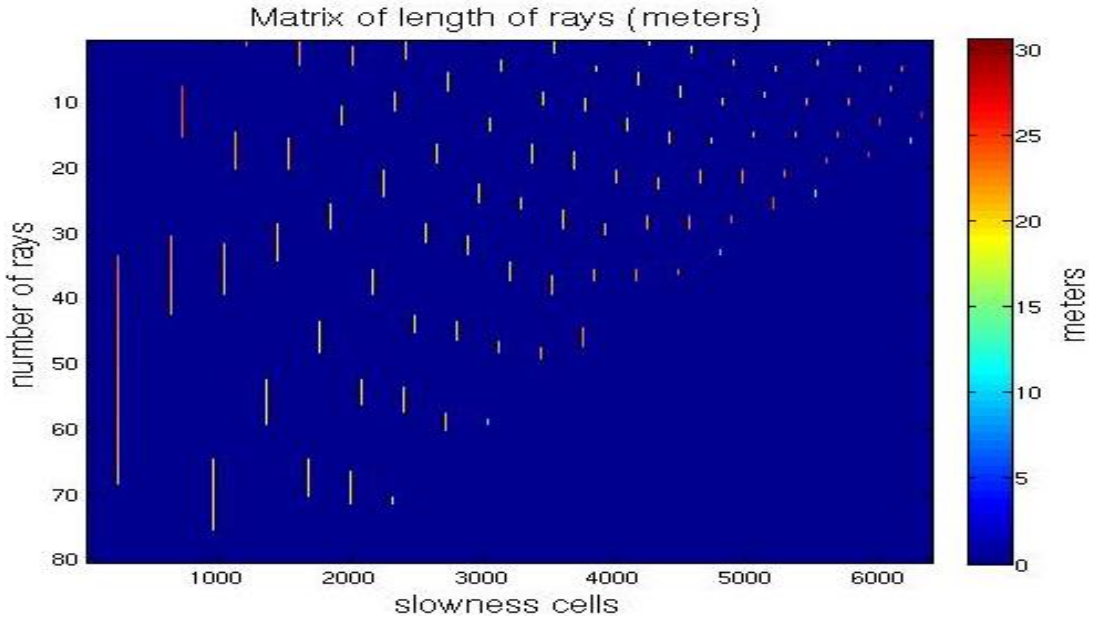


FIG 11. The matrix of lengths of raypaths for shot number 1.

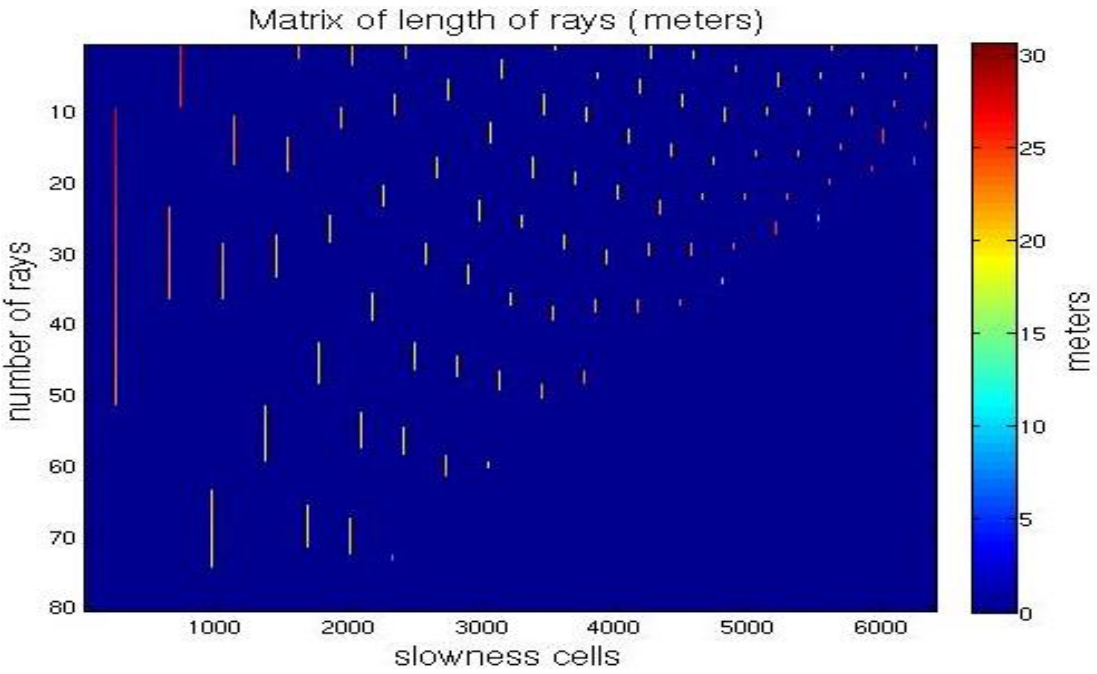


FIG 12. The matrix of lengths of raypaths for shot number 2.

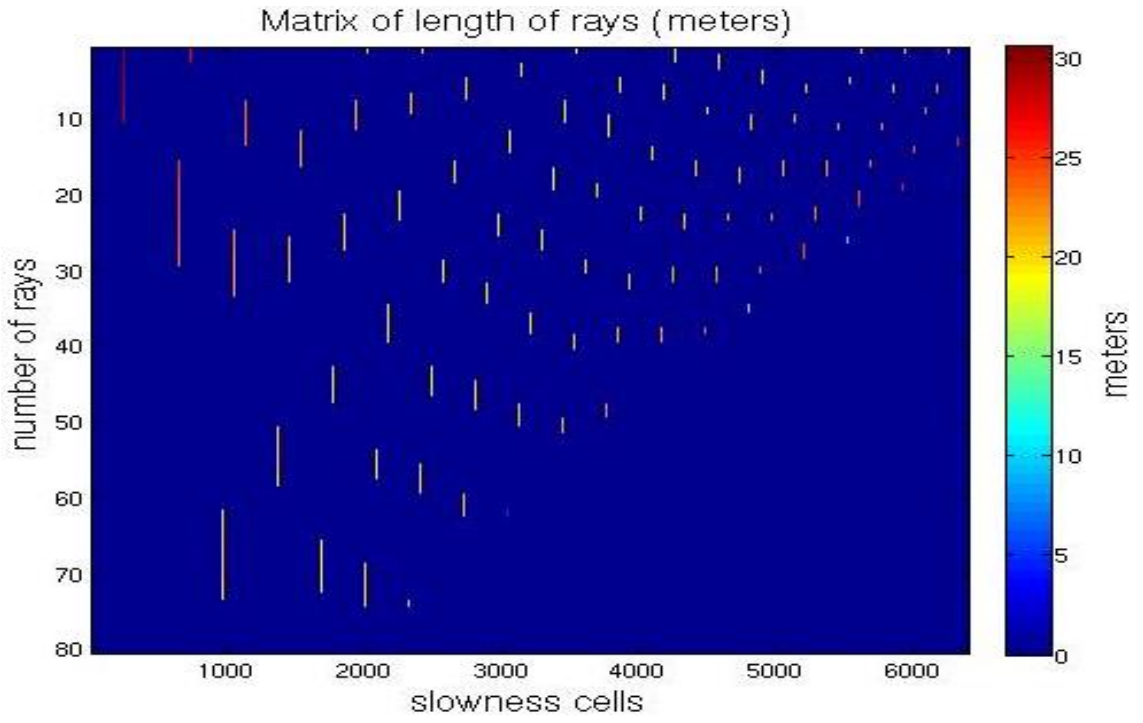


FIG 13. The matrix of lengths of raypaths for shot number 3.

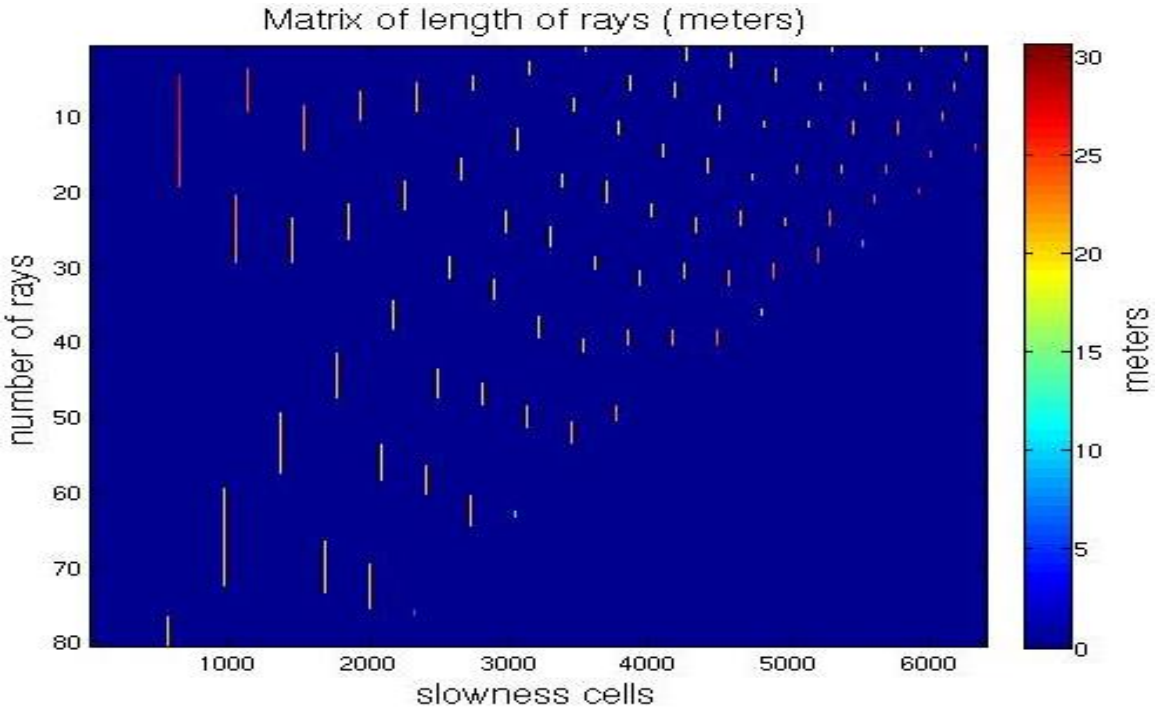


FIG 14. The matrix of lengths of raypaths for shot number 4.

## CONCLUSIONS AND DISCUSSIONS

We have developed a turning-ray tracing algorithm for a linear velocity v(z) medium that uses Slotnick's equations. For the four shots we tested, the calculated traveltimes

from turning-ray tracing match the traveltimes generated using finite-difference modelling. Shot number 4 does not quite match the traveltimes from finite-difference modelling, however will investigate this by ray tracing with several shots.

The accuracy of the matrices of the lengths of raypaths will be tested when we solve the inverse problem of estimating the slowness. This will be the focus of our subsequent paper.

## ACKNOWLEDGEMENTS

We thank the sponsors of CREWES for their support. We also gratefully acknowledge support from NSERC (Natural Science and Engineering Research Council of Canada) through the grant CRDPJ 379744-08.

## REFERENCES

Arenrin, B.I., Margrave, G. F., Bancroft, J., 2014; Application of turning-ray tomography to Hussar 2D seismic line from central Alberta, SEG Technical Program Expanded Abstracts 84. 4827-4831.

Epili, D., Criss, J., Cunningham, D., 2001; Turning-Ray Tomography for Statics Solution,63th EAGE conference & Exhibition.

Langan R.T., Lerche I., Cutler R.T., Bishop T.N., Spera N.J., 1984; Seismic tomography; The accurate and efficient tracing of rays through heterogeneous media, SEG Technical Program Extended Abstracts, 713-715.

Margrave, G. F., Methods of Seismic Data Processing, Geophysics 517, pages 6-25, 6-26 Department of Geology and Geophysics, University of Calgary.

Padina, S., Churchill, D., Bording, R.P., 2006; Travel time inversion in seismic tomography. Available from http://webdocs.cs.ualberta.ca/~cdavid/pdf/HPCSPaper.pdf [Accessed 11/11/2014]

Promax, 1997; A reference guide for the Promax geophysical processing software, Landmark graphics corporation.

Slotnick, M.M.,1959; Lessons in Seismic Computing, SEG

Stefani, J.P., 1995; Turning-ray tomography, Geophysics 60, 1917-1929.

Yilmaz, OZ., 2001; Seismic data analysis; Investigation in geophysics, **1.**

Zhu, X., Sixta, D. P., Angstman, B. G., 1992; Tomostatics: Turning-ray Tomography + Static Corrections, The Leading Edge **11**, no. 12, 15-23.

Zhu,T., Cheadle, S., Petrella, A., Gray, S., 2001; First-arrival tomography for near surface model building Tomography, **63rd** EAGE conference & Exhibition.